Scientific Research Publishing

Journal of Cancer Therapy, 2023, 14, 182-201
https://www.scirp.org/journal/jct
ISSN Online: 2151-1942
ISSN Print: 2151-1934

MIR-448 Regulates MAGEA6/AMPK Signaling Pathway in Hepatocellular Carcinoma Tumor Stem Cells

Changliang Jiao[1], Jinfang Zheng[2], Juncheng Guo[3]

[1]Hainan Vocational University of Science and Technology, Haikou, China
[2]Hainan Provincial People's Hospital, Haikou, China
[3]Haikou Hospital, Xiangya School of Medicine, Central South University, Haikou, China
Email: g2002m@163.com

How to cite this paper: Jiao, C.L., Zheng, J.F. and Guo, J.C. (2023) MIR-448 Regulates MAGEA6/AMPK Signaling Pathway in Hepatocellular Carcinoma Tumor Stem Cells. *Journal of Cancer Therapy*, **14**, 182-201.
https://doi.org/10.4236/jct.2023.144017

Received: March 31, 2023
Accepted: April 25, 2023
Published: April 28, 2023

Abstract

Objective: To explore the role of miR-448 in regulating MAGEA6/AMPK signaling pathway in the biological study of hepatocellular carcinoma (HCC) tumor stem cells. **Methods:** Using the database, the hepatocellular carcinoma related expression chips were obtained and the regulatory mirnas of candidate genes were predicted, and the predicted results were analyzed. The effects of miR-448 and MAGEA6 on the pellet formation rate and clone formation rate of hepatocellular carcinoma stem cells were detected by immunofluorescence identification of stem cell markers and light microscope counting method. The effects of miR-448 and MAGEA6 on migration and invasion of hepatocellular carcinoma stem cells were detected by scratch and Transwell assay. Dual luciferase reporter assay to verify whether miR-448 targets MAGEA6. The expression and influence of miR-448 on MAGEA6 and AMPK pathway were detected by qRT-PCR and Western blot. **Results:** It was found that miR-448 may directly regulate the expression of MAGEA6. Overexpression of miR-448 inhibited the characteristics, proliferation, migration, and invasion of hepatocellular carcinoma stem cells *in vitro*, as well as the ability of xenograft tumor formation *in vivo*. However, inhibition of miR-448 showed opposite results. In addition, miR-448 directly targets MAGEA6 and regulates AMPK signaling. Silencing MAGEA6 and adding AMPK activator further verified that miR-448 activated AMPK signaling pathway by targeting MAGEA6, thus affecting characteristics, proliferation, migration and invasion of hepatoma stem cells. **Conclusions:** Our results reveal that miR-448 activates AMPK signaling pathway by targeting MAGEA6, thereby affecting characteristics, proliferation, migration and invasion of hepatoma stem cells. It is suggested

that overexpression of miR-448 may be a new therapeutic strategy for hepatocellular carcinoma.

Keywords

mir-448, MAGEA6, AMPK Signaling Pathway, Liver Cancer, Tumor Stem Cells

1. Introduction

Hepatocellular carcinoma (HCC) is a common malignant tumor, and the invasion and metastasis of tumor cells is one of the important reasons why it is difficult to cure, among which tumor stem cells are the focus of this study [1]. In previous studies, MAGEA6 was confirmed to be involved in the invasion and metastasis process of HCC stem cells. Through GEO data analysis and biogenic prediction, the upstream gene miR-448 of MAGEA6 was screened out. Overexpression of miR-448 could reduce the expression of MAGEA6. The expression of miR-488 regulating p-AMPK protein was further found in tumor stem cells of HCC patients [2] [3] [4] [5]. Based on this, we proposed a scientific hypothesis that miR-448 activates AMPK signaling pathway by targeting MAGEA6, thus affecting the biological function of liver cancer stem cells [6] [7]. We will further explore the effects of miR-448 in HCC on invasion and metastasis through regulation of MAGEA6/AMPK signaling pathway at the cellular, tissue and animal levels, providing new ideas for exploring therapeutic approaches to HCC.

2. Experimental Methods

2.1. Chip Analysis and Regulation of miRNA Prediction

Using GEO database (https://www.ncbi.nlm.nih.gov/geo/), the retrieval express chip for hepatocellular carcinoma (HCC). Using R language "limma" package to $|\log FC| > 2$, p value < 0.05 for differences in gene screening criteria. Differential gene expression was constructed using pheatmap package. Using TargetScan (http://www.targetscan.org/vert_71/), database StarBase database (http://starbase.sysu.edu.cn/), MiRSearch database , MirDIP database (https://ophid.utoronto.ca/mirDIP/index.jsp#r) and DIANA database, the regulation miRNA of MAGEA6 was predicted, and the intersection of prediction results was taken.

2.2. Culture of liver cancer cells

Human hepatocellular carcinoma line Hep3B and hepatocellular carcinoma line L02 were obtained from the U.S. Typical Culture Preservation Center (ATCC; Manassas, VA, USA, http://www.atcc.org), cultured in DMEM medium containing 10% fetal bovine serum (HyClone, Logan, UT), 100 U/mL penicillin, and 100 U/mL streptomycin, incubated in a humid incubator at 37˚C with 5% CO_2.

2.3. Screening and Identification of Hepatocellular Carcinoma Stem Cell-Like Cells

Harvested cells were washed twice with PBS containing 2% heat-inactivated FBS and re-suspended in a cell staining buffer (BioLegend, San Diego, CA) at a concentration of 10^7 cells/ml. Cell suspension was incubated with PE-CD133 (Miltenyi Biotec) and FITC-CD44 (eBioscience) or isotype control antibodies PE-IgG and FITC-IgG (eBioscience) at 4˚C for 30 min. The sample was then washed twice with PBS/ 2% FBS and then cell sorted the stained cells using BD Immunocytometry Systems (San Jose, CA).

2.4. Detection of Surface Marker Molecules of Liver Cancer Stem Cells

The sorted cells were cultured for 48 h to detect the expression of Sarbox-2 and OCT-4, and fixed at 4˚C for 10 min with 4% paraformaldehyde. The cells were washed with PBS and sealed with 10% serum from PBS containing 0.5% Triton X-100. The cells were then treated at 4˚C with a mouse anti-human antibody Sarbox-2 (1:200, ab171380, Abcam, Cambridge, MA, USA), and primary antibody of rabbit anti-human antibody OCT-4 (1:1000, ab208272, Abcam, Cambridge, MA, USA) were incubated overnight. The cells were then washed with PBS three times. Appropriate Alexa Fluor555 fluorine-labeled second antibodies were added to cells and incubated at 37˚C for 1 h. Isotype IgG serves as a non-specific control. The nuclei were re-stained with 4', 6-diaminyl-2-phenylindole (DAPI) contained in a fixative (Vector Labs) and observed under a fluorescence microscope (Olympus XF-73).

2.5. Double Luciferase Reporting Experiment

Synthesis of miR-448 to predict the 3'-UTR of MAGEA6 containing putative binding sites (Integrated Biotech Solutions Co., Ltd., Shanghai, China), It was placed at the XbaI site of pGL3 vector (Promega, Madison, WI) and named pgl3-Magea6-3'-UTR-WT. Accordingly, a luciferase reporter gene MAGEA6 MUT containing mutant sequences at the binding site of miR-448 was constructed, and finally named pGL3-MAGEA6-3'-UTR-WT-MUT. HCC stem cells were inoculated into a 24-well plate (1.5×10^5 cells/well) 24 hours before transfection. And then, Transfected 80 ng pRL-TK Renilla (Promega) plasmid with Lipofectamine 2000 (Invitrogen) reagent into 60 pmol miR-448-mimic or miRNA mimic according to the manufacturer's protocol control and 200 ng pGL3-MAGEA6-3'-UTR-WT or pGL3-MAGEA6-3'-Utr-wt-mut cotransfected cells. The Dual Luciferase Reporter Assay System (Promega Corporation, Madison, WI, USA) was used to measure luciferase activity 48 h after transfection. Firefly luciferase activity was normalized to sea kidney luciferase activity for each transfected well.

2.6. Cell Transfection and Grouping

miR-448 mimic group, NC mimic group, miR-448 inhibitor, NC inhibitor,

si-MAGEA6 group, si-NC group were all purchased from GenePharma Co., Ltd., (China) for cell transfection. Liver cancer stem cells were inoculated in 6-well plates and transfected with different plasmids using Lipofectamine2000 (Invitrogen) reagent according to the instructions [5].

AMPK pathway activator group was treated with 0.5 mmol/l AICAR [6] (5-aminoimidole-4-carboxamide-1-β-D-Ribofuranoside, St. Louis, MO) for 48 h.

2.7. Experiment on Formation of Suspended Clonal Cell Spheres

The cells were inoculated in 6-well ultra-low adhesion plates (Corning Inc., Corning, NY, USA) at a density of 1×10^3 cells/mL. DMEM/F12 serum-free medium (Invitrogen) with 2 mM L-glutamine, 1% sodium pyruvate (Invitrogen), 100 μg/ml penicillin G, and 100U/ml streptomycin supplemented with 20 ng/ml epithelial growth factor (Invitrogen), 10 ng/ml fibroblast growth Factor-2 (Invitrogen), N2 (Invitrogen) and B27 (Invitrogen). HCC cells were incubated in a CO_2. incubator for 1 - 2 weeks, and many balloon cells were counted under a stereo microscope (Olympus, Tokyo, Japan). Only the number of tumor ball cells larger than 50 μm in diameter was counted.

2.8. Soft AGAR Colony Formation Experiment

Liver cancer stem cells were harvested and suspended in culture medium. 1 ml 0.5% agarose (Invitrogen) was added to the 6-well plate and gelled at room temperature to prepare the substrate. The top layer (0.25% agarose) was prepared by mixing 500 μl 0.5% agarose with 500 μl cell suspension containing 5000 cells. The mixture is coated over the bottom layer and allowed to cure at room temperature. After solidification, another 2 ml medium was added to the top layer and the cells were incubated at 37˚C 5% CO_2 for 3 weeks. Four weeks after growth, the cells (Leica Microsystems Imaging Solutions Ltd., Cambridge, UK) were immobilized with ethanol, stained with 0.1% crystal violet (C0004, Baomanbio), and photographed. The number of clones was counted using ImageJ software, and the data was expressed as the mean ± standard deviation of the five random scoring areas.

2.9. Transwell Experiment

Cell invasion assay was performed in 24-well Transwell plate (aperture, 8 μm; Corning Incorporated, Corning, NY, USA). Cells (1×10^5) were re-suspended in 200 μl serum-free medium and placed in the upper chamber. 500 μl serum containing 20% FBS was added to the lower chamber. The polycarbonate film in the upper chamber was pre-coated with Matrigel (diluted, 1:3; BD Biosciences, San Jose, CA, USA). After incubating at 37˚C with 5% CO_2, for 48 h, the matrix glue and cells in the upper chamber were wiped off with cotton swabs, the invading cells in the lower chamber were fixed with methanol, and stained with 0.1% crystal indigo (C0004, Baomanbio) at room temperature for 30 min. Finally, cells were photographed at ×20 magnification using a Leica DC 300F positive microscope

(Leica Microsystems Imaging Solutions Ltd., Cambridge, UK) and counted using the ImageJ software.

2.10. Scratch Test

Cells (5×10^5) were inoculated in 6-well plates and grew in medium until cells were 90% fused in DMEM medium containing FBS. A 1 mm wide scratch was then made using the sterile 200 μl pipette tip across the entire cell layer. The isolated cells were washed away with PBS. After the scratch, a new medium was added for another 24 h culture. 0 h and 24 h after the scratch, the photos were taken at the same position, and the scratch width (W) was measured. The method of calculating the migration distance of cells was the scratch width at 0 h time point minus the scratch width at 24 h time point.

2.11. QRT-PCR

According to the manufacturer's instructions, TRIzol reagents (Invitrogen, Carlsbad, CA, USA) and mirVana™ miRNA Isolation Kit (Invitrogen, USA)otal RNA was extracted from tissues or cultured cells. Using PrimeScript RT kit (Takara, Dalian, Liaoning, China) and miRNA Reverse Transcription Kit TaqMan® MicroRNA Reverse Transcription Kit (Applied Biosystems, USA) The concentration and purity of RNA samples were determined by spectrometric method. qRT-PCR was performed using SYBR Prime Script RT-PCR kit (Takara, Japan) based on the manufacturer's instructions. Using GAPDH and U6 mRNA as internal parameters, primer sequences for quantitative real-time PCR are shown in the Table 1. Each experiment was repeated three times, and $2^{-\Delta\Delta CT}$ was used to assess differences in expression levels [8] [9].

2.12. Western Blot

Cells cultured for 48 h were ground with RIPA (radioimmunoprecipitation, Sangon Biotech, China) lysate containing PMSF (phenylmethane fluoride, Sigma, USA), then centrifuged at 4˚C at 12,000 rpm for 10 min. The supernatant was collected and the protein concentration of each sample was determined using a BCA

Table 1. Primer sequence.

Primer	Sequence
miR-448 [10]	forward: 5'-TTATTGCGATGTGTTCCTTATG -3' reverse: 5'-ATGCATGCCACGGGCATATACACT-3'
GAPDH [11]	forward: 5'-AGAAGGCTGGGGCTCATTTG-3' reverse: 5'-AGGGGCCATCCACAGTCTTC-3'
U6 [10]	forward: 5'-CGCTTCGGCAGCACATATACTAAAATTGGAAC-3' reverse: 5'-GCTTCACGAATTTGCGTGTCATCCTTGC-3'
MAGEA6 [11]	forward: 5'-AAAGGCAGAAATGCTGGGGAG-3' reverse: 5'-AGGCAGGTGGCAAAGATGTACAC-3'

protein assay kit (Pierce, Rochford, IL). The proteins were isolated on 10%SDS-PAGE gel (sodium dodecyl sulfate-polyacrylamide gel electrophoresis, Comiike, China) and then transferred to polyethylene fluoride (PVDF) membranes (Mippore, USA) [12]. The membrane was sealed at room temperature for 1 h in Tris buffered saline (TBST) containing 5% skim milk, then a primary antibody MAGEA6 (1:100, ab38495, Abcam, Cambridge, MA, USA) was added. p-AMPKα (Thr172) (40H9) (1:1000, #2535, Cell Signaling Technology Inc., Danvers, MA, USA), AMPKα(1:1000, ab32047, abcam, Cambridge, MA, USA), CD133 (1:1000, ab16518, abcam, Cambridge, MA, USA), SOX-2 (1:1000, ab92494, abcam, Cambridge, MA, USA), OCT-4 (1:1000, ab181557, abcam, Cambridge, MA, USA), Nanog (1:1000, ab80892, abcam, Cambridge, MA, USA). Incubate overnight at 4˚C. Goat anti-Rabbit IgG (1:2000, ab6721, Abcam, Cambridge, MA, USA) labeled with horseradish peroxidase was then incubated at room temperature for 1 h. Finally, the PVDF membrane was washed with 1 × TBST buffer solution for 10 minutes, three times in total. The film was immersed in the ECL reaction for color development, and the cassette was exposed for development. GAPDH is the internal parameter. The gray values of protein bands were analyzed by ImageJ software. The relative gray values of target bands and internal reference bands were the relative expression levels of protein.

2.13. Tumor Xenograft Tumor Model

6-week-old BALB/c nude mice were randomly divided into 2 groups (n = 12 per group) with body weight of 18 - 22 g and were treated with miR-448-Agomir or Agomir negative control (GenePharma, Shanghai, Hep3B CD133+ cells (5×10^6) transfected in China were injected subcutaneously into the right side of nude mice. The tumor volume was measured using an external caliper and calculated using the equation (L × W2)/2. Tumor growth was monitored every 4 days and the mice were killed after 4 weeks to measure tumor weight. All experimental procedures are approved by the Animal Ethics Committee.

2.14. Statistical Analysis

SPSS 21.0 statistical software was used for analysis. χ^2 test was used for categorical variables, and t test for two independent samples was used for normally distributed continuous variables. $P < 0.05$ was considered statistically significant.

3. Experimental Results

3.1. Hepatocellular Carcinoma Related Gene Screening and miRNA Prediction

GEO database was used to retrieve the hepatocellular carcinoma expression chip GSE40367 (10 samples were primary HCC tumors, 12 samples were HCC with lung metastasis). The differential expression analysis of the chip showed that 26 differentially expressed genes were obtained, and the expression level of 19 genes in the tumor group was significantly improved. The expression levels of 7 genes

in the control group were significantly increased. Among these differentially expressed genes, we noticed that the three genes with the largest differentially expressed changes in tumor samples were ACOT12, MAGEA6 and PSMD8. Among the three genes, ACOT12 and PSMD8 are rarely studied in hepatocellular carcinoma and tumor diseases, while MAGEA6 has a very few literatures indicating that it may be closely related to the development of hepatocellular carcinoma [13] [14]. Moreover, studies have found that MAGEA6 can promote the development of tumor diseases and is highly expressed in tumors. In the GSE40367 chip, MAGEA6 was also highly expressed in the tumor group. Moreover, studies have found that MAGEA6 gene can regulate the development of tumors through AMPK signaling pathway [15]. These analysis results and literature reports suggest that MAGEA6 may function through AMPK signaling pathway in hepatocellular carcinoma. In order to further understand the upstream regulatory mechanism of MAGEA6 gene, TargetScan and other databases were used to predict the regulatory miRNA of MAGEA6, and the intersection of the predicted results was found that only one miRNA, miR-448, existed in the intersection set of the predicted results of five different databases (**Figure 1**). This suggests that miR-448 may affect the development of hepatocellular carcinoma by targeting the MAGEA6 gene.

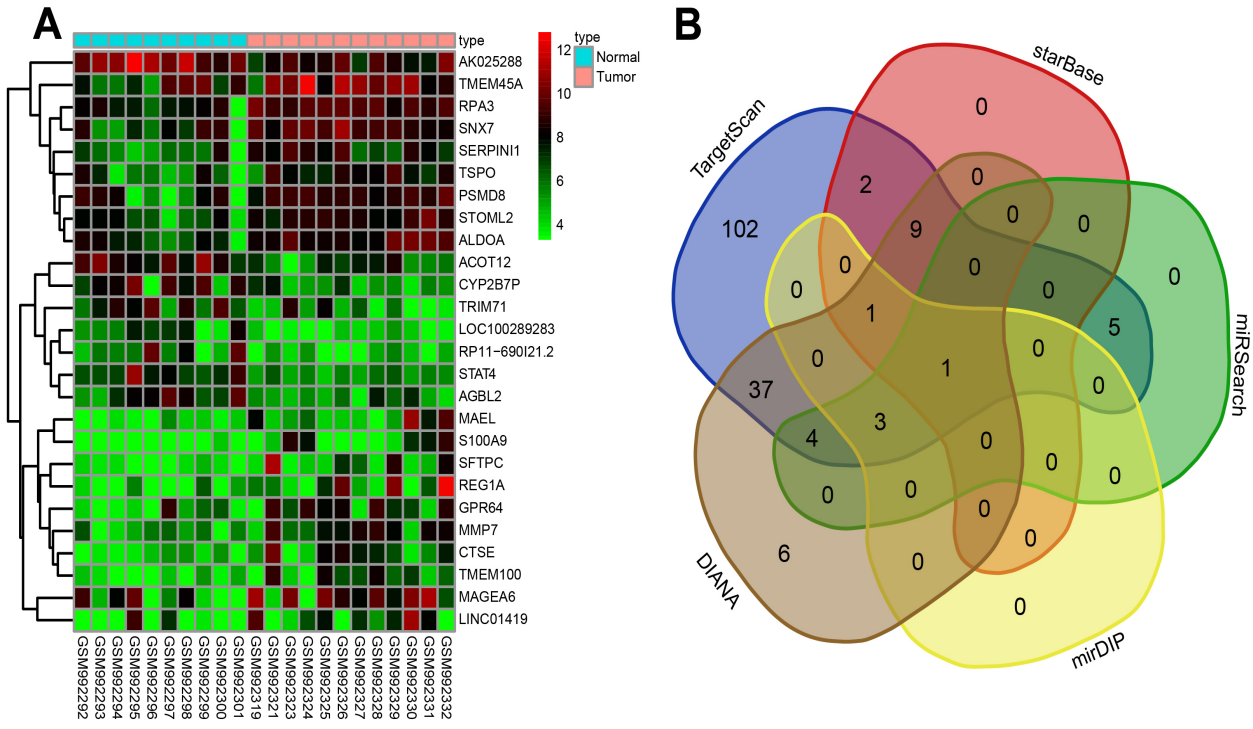

Figure 1. Differential analysis of hepatocellular carcinoma expression microarray and prediction of regulatory miRNA. (A) Differential gene expression heat map of hepatocellular carcinoma chip, horizontal coordinate represents sample number, vertical coordinate represents gene name, tree diagram on the left represents gene expression level clustering, each small square in the figure represents the expression level of a gene in a sample, histogram on the upper right is color level. (B) MAGEA6 regulates miRNA prediction. The five irregular figures in the figure respectively represent the prediction results of MAGEA6 regulates miRNA from five different databases, and the middle part is the intersection of the prediction results of five databases.

3.2. Sorting of Hepatocellular Carcinoma Tumor Stem Cells

Hepatocellular carcinoma stem cells (CD133+CD44+) were sorted by cell sorting flow cytometry, and the expression of stem cell markers of the screened CD133+CD44+ hepatocellular carcinoma stem cells was detected by immunofluorescence. The results showed that Sarbox-2 and OCT-4 were highly expressed in the cells.

In order to verify the expression of MAGEA6 in Hep3B, qRT-PCR was used to detect the expression of MAGEA6 mRNA in L02, CD133-CD44-cells of normal liver cells and CD133+CD44+ liver cancer stem cells. The results showed that: Compared with normal hepatocytes L02, MAGEA6 mRNA in CD133-CD44-hepatoma cells and CD133+CD44+ hepatoma stem cells was significantly increased ($P < 0.05$). MAGEA6 mRNA in CD133+CD44+ hepatoma stem cells was significantly increased compared with CD133-CD44- hepatoma cells ($P < 0.05$) (**Figure 2**).

3.3. MAGEA6 Silencing Can Inhibit the Pellet Formation, Colony Formation and Invasion and Migration Ability of Hepatoma Tumor Stem Cells

In order to select an effective plasmid that could interfere with MAGEA6 expression, mRNA expression of MAGEA6 in hepatocellular carcinoma stem cells was detected by RT-qPCR after transfection of siRNA1, siRNA2 and siRNA3. The results showed that mRNA expression of MAGEA6 decreased after transfection with siRNA1, siRNA2 and siRNA3 plasmids compared with NC plasmids, and the transfection efficiency of siRNA1 was the highest. Therefore, siRNA1 is selected as the interference sequence of MAGEA6 due to its best efficiency [16] [17]. Next, cells were treated with si-MAGEA6 or AICAR (activator of AMPK signaling pathway) to investigate the effects of MAGEA6 and AMPK signaling pathways on sphere formation, colony formation, invasion and migration of hepatocellular carcinoma stem cells. Compared with the si-NC group, the results showed that the pellet-forming ability of liver cancer in si-MAGEA6 and AICAR groups was significantly decreased ($P < 0.05$). Compared with si-NC group, colony formation ability of si-MAGEA6 group and AICAR group was significantly decreased ($P < 0.05$). Scratch test showed that cell migration ability in si-MAGEA6 and AICAR groups was significantly decreased compared with si-NC group ($P < 0.05$). Transwell experiment showed that the cell invasion ability of si-MAGEA6 group and AICAR group was significantly decreased compared with that of si-NC group ($P < 0.05$). WB test results showed that: Compared with the si-NC group, the expression of AMPK in si-MAGEA6 and AICAR groups had no significant changes, the protein level of P-AMPK was significantly increased, and the protein expressions of Sox4, Oct4 and Nanog were significantly decreased (all $P < 0.05$). The results indicated that MAGEA6 negatively regulated AMPK activity (**Figure 3**). These results suggest that silencing MAGEA and activating AMPK signal can inhibit pellet formation, colony formation, invasion and migration of hepatoma tumor stem cells.

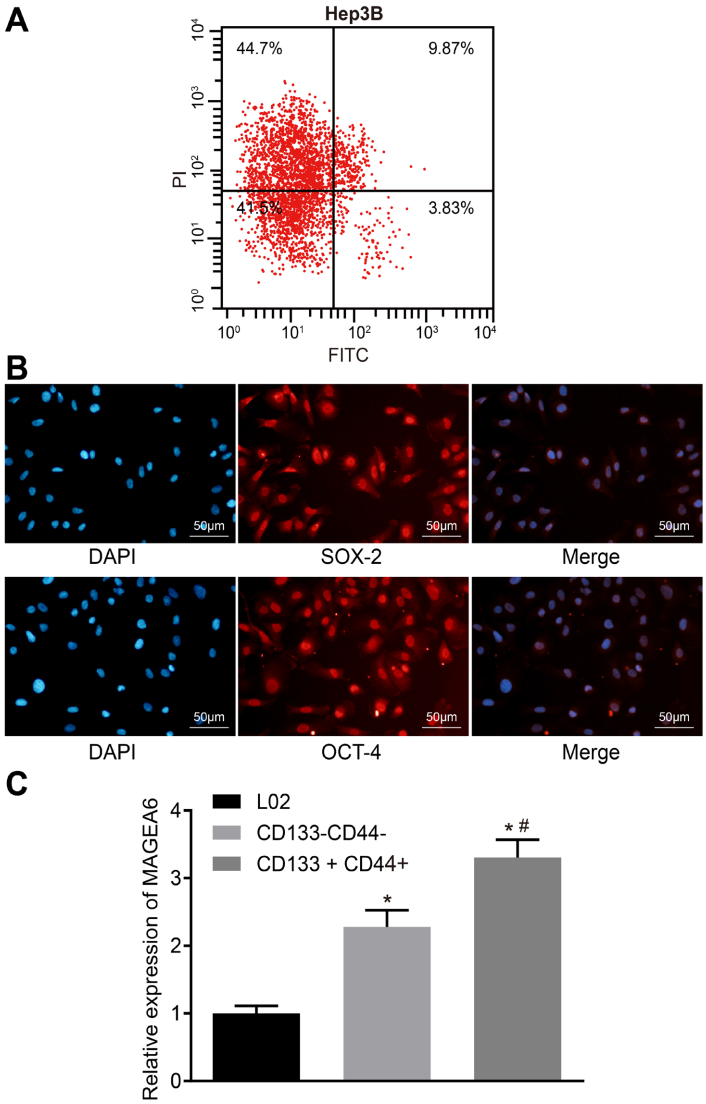

Figure 2. (A) Flow cytometry for HCC stem cells (CD133+CD44+); (B) Hep3B CD133+CD44+ stem cell markers were detected by immunofluorescence staining; (C) The expression of MAGEA6 mRNA in L02, CD133-CD44-liver cancer cells and CD133+CD44+ liver cancer stem cells of normal liver cells was detected by qRT-PCR. The data in the figure were measurement data, expressed as mean ± standard deviation. Independent sample t test was used for comparison between the two groups, and the experiment was repeated three times. * meant $P < 0.05$ compared with L02, and # meant $P < 0.05$ compared with CD133-CD44-hepatoma cells.

3.4. miR-448 Targeted Inhibition of MageA6-Mediated AMPK Signaling Pathway

In order to understand the upstream regulation mechanism of MAGEA6, the Targetscan database was used to predict MAGEA6 targets. The 3'-UTR of MAGEA6 contains the putative binding sequence of miR-448 [18]. In order to study the correlation between miR-448 and MAGEA6, luciferase reporting detection was conducted to verify whether MAGEA6 was the target of miR-448. We cloned the wild type (WT) of MAGEA6 and the mutant 3'-UTR into the

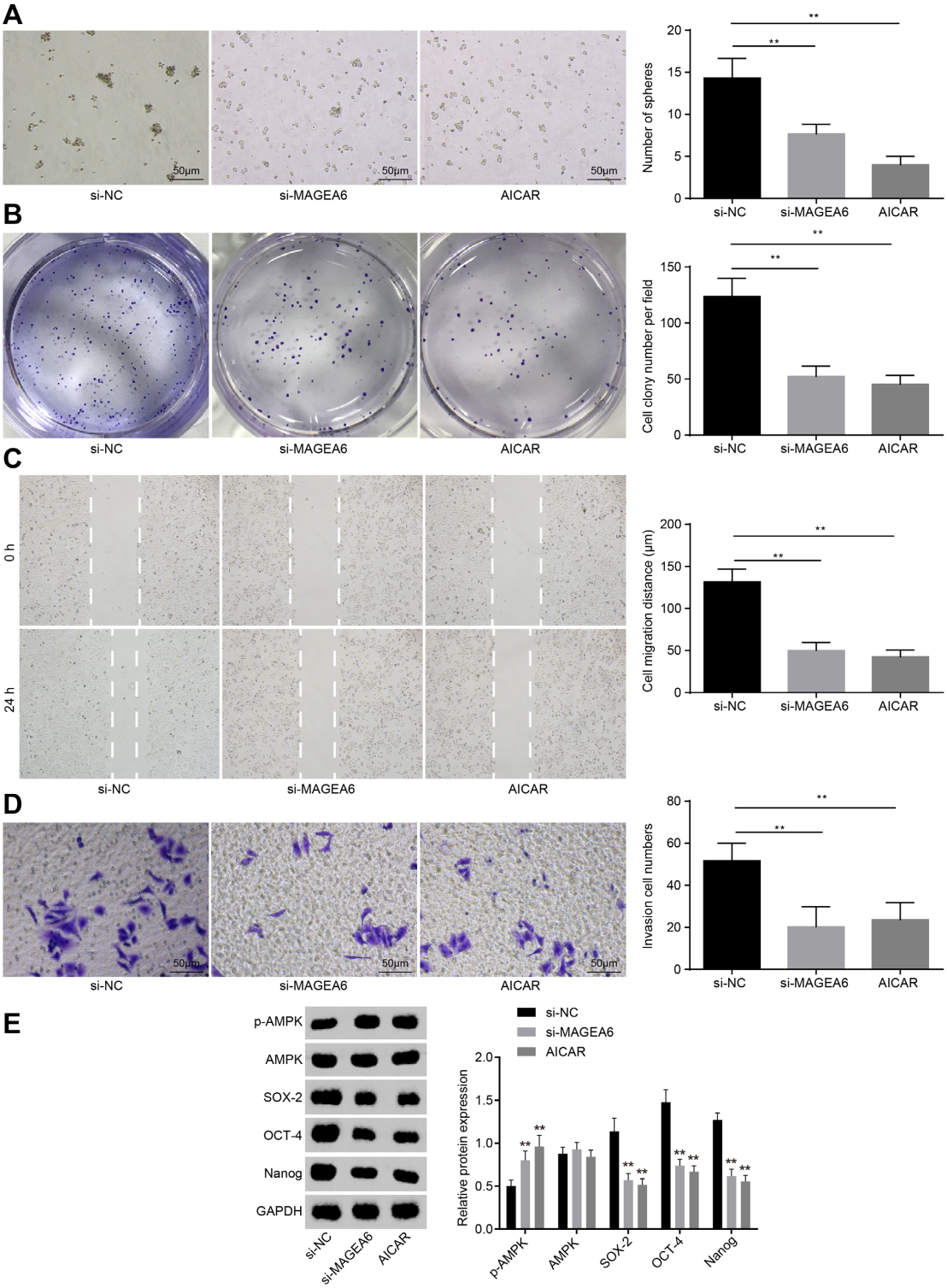

Figure 3. MAGEA6 silencing inhibits pellet formation and invasion and migration of hepatocellular carcinoma stem cells. Note: (A) Test result of stem cell pellet formation (×200); (B) clone formation test results; (C) Cell migration was detected by scratch test; (D) Transwell was used to detect cell invasion (×200). E: WB was used to detect the expression of AMPK signaling pathway related proteins and Sox4, Oct4 and Nanog proteins in liver cancer stem cells. Based on three independent experiments, the data were expressed as mean ± standard deviation. Independent sample t test was used for comparison between the two groups, and ** means $P < 0.05$ compared with NC.

pmirGLO plasmid, respectively. Ppmir-magea6-wt and PPMIR-Magea6-mut transfected liver cancer stem cells using miR-448 mimic. The luciferase activity of pmirGLO-MAGEA6-WT group was significantly lower than that of pmirGLO-MAGEA6-MUT group ($P < 0.05$), indicating that miR-448 can bind MAGEA6 specifically. In addition, qRT-PCR and western blot confirmed that MAGEA6 mRNA and protein expression levels of miR-448 mimic cells were significantly reduced, and P-AMPK protein expression levels were increased after liver cancer stem cells with NC mimic group ($P < 0.05$). In addition, compared with NC inhibitor group, miR-448 inhibitor significantly increased MAGEA6 mRNA and protein expression levels, and decreased P-AMPK protein expression levels ($P < 0.05$). These results indicated that miR-448 could target MAGEA6 binding and inhibit MAGEA6 expression, thus activating AMPK signaling pathway (Figure 4).

3.5. Overexpression of miR-448 Can Inhibit the Effects of Pellet Formation, Colony Formation and Invasion and Migration of Hepatoma Tumor Stem Cells

The results showed that the pellet-forming ability of liver cancer stem cells was

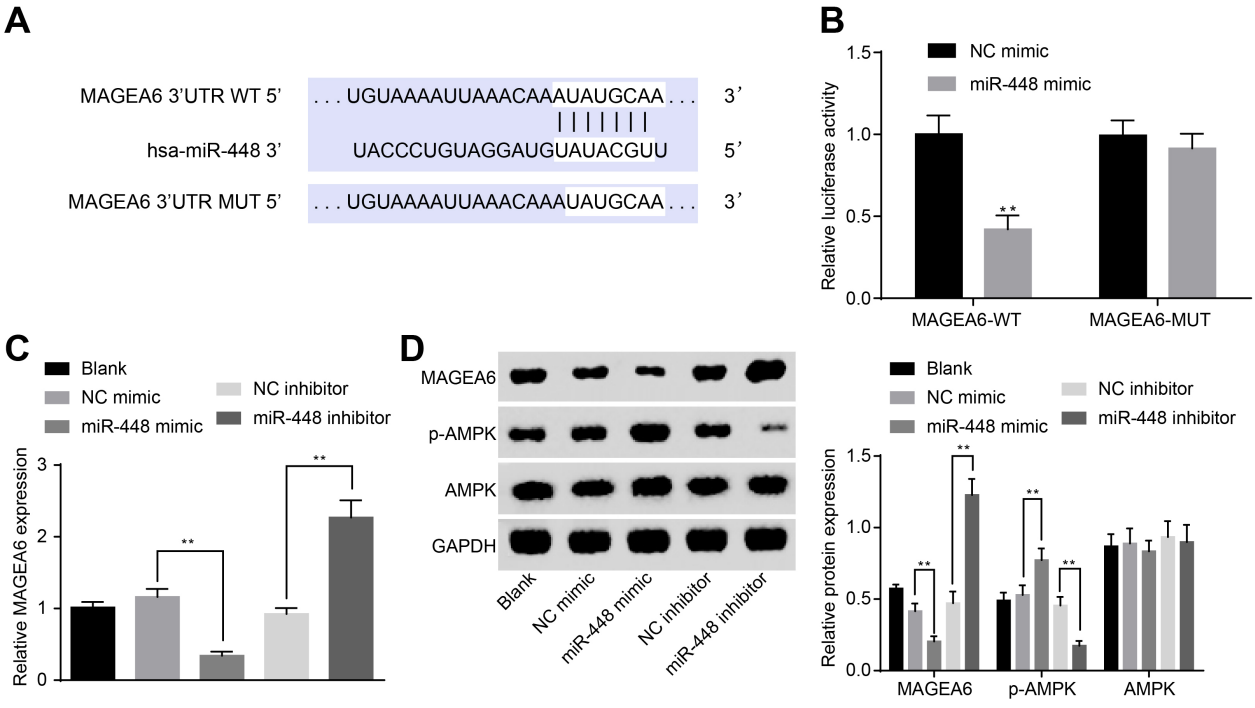

Figure 4. miR-448 targets the MageA6-mediated AMPK signaling pathway. Note: (A) WT and MUT sequences designed for MAGEA6 according to the binding site of miR-448; (B) The relative activity of luciferase after co-transfection with miR-448 mimic with Pmirgloo-Magea6-wt or Pmirgloo-Magea6-Mut was detected by dual luciferase assay. (C) qRT-PCR was used to detect MAGEA6 mRNA expression in hepatoma stem cells. (D) The expression of MAGEA6 and AMPK signaling pathway related proteins in hepatoma stem cells was detected by WB. Based on three independent experiments, the data were expressed as mean ± standard deviation. The comparison between the two groups was analyzed by the independent sample t test statistical method, and the comparison between the multiple groups was analyzed by the single factor variance statistical method. ** indicates $P < 0.05$ compared with NC.

significantly decreased after miR-448 mimic group compared with NC mimic group, while the pellet-forming ability of liver cancer stem cells was significantly increased after miR-448 mimic group compared with NC inhibitor group ($P < 0.05$). The clone formation experiments showed that miR-448 mimic group significantly reduced colony formation ability compared with NC mimic group, while miR-448 inhibitor group significantly enhanced colony formation ability compared with NC inhibitor group ($P < 0.05$). Scratch test showed that the cell migration ability of miR-448 mimic group was weakened compared with NC mimic group, while the cell migration ability of miR-448 inhibitor group was enhanced compared with NC inhibitor group ($P < 0.05$). Transwell experiments showed that the cell invasion ability of miR-448 mimic group was significantly reduced compared with NC mimic group, while the cell invasion ability of miR-448 inhibitor group was significantly enhanced compared with NC inhibitor group ($P < 0.05$). WB test results showed that: The protein expressions of Sox4, Oct4 and Nanog were significantly decreased after miR-448 mimic group compared with NC mimic group (all $P < 0.05$), but compared with NC inhibitor group, Protein expressions of Sox4, Oct4 and Nanog were significantly increased in miR-448 inhibitor group ($P < 0.05$). Therefore, miR-448 can inhibit the pellet formation, colony formation, invasion and migration of hepatoma tumor stem cells (**Figure 5**).

3.6. Rescue Experiment Verification

In order to investigate whether miR-448 plays its biological function through MAGEA6, rescue experiments were conducted by inhibiting the expression of miR-448 in MAGEA6 knockout hepatoma cells. Stem-cell pellet formation experiment showed that miR-448 inhibitor + si-MAGEA6 group could reverse the maintenance effect of miR-448 inhibitor group on pellet-forming properties of hepatoma stem cells ($P < 0.05$). Clonal formation experiment showed that miR-448 inhibitor + si-MAGEA6 group could reverse the promoting effect of miR-448 inhibitor group on colony formation ability of hepatoma stem cells ($P < 0.05$). Scratch and Transwell experiments showed that miR-448 inhibitor + si-MAGEA6 inhibitor group could reverse the promoting effect of miR-448 inhibitor group on migration and invasion ability of hepatoma cells ($P < 0.05$). WB experiment showed that miR-448 inhibitor + si-MAGEA6 group could reverse the inhibition effect of miR-448 inhibitor group on AMPK signal ($P < 0.05$). In general, MAGEA6 silencing could reverse the effects of miR-448 inhibitor on tumor stem cell pellet formation and colony-forming ability and invasion and migration ability (**Figure 6**).

3.7. miR-448 Inhibits Tumor Formation and Stem Cell Properties *in Vivo*

In order to investigate whether miR-448 is associated with tumor growth, mouse xenograft tumor formation test was conducted. Compared with Agomir NC group, the xenograft tumors in miR-448-Agomir group were smaller and lighter

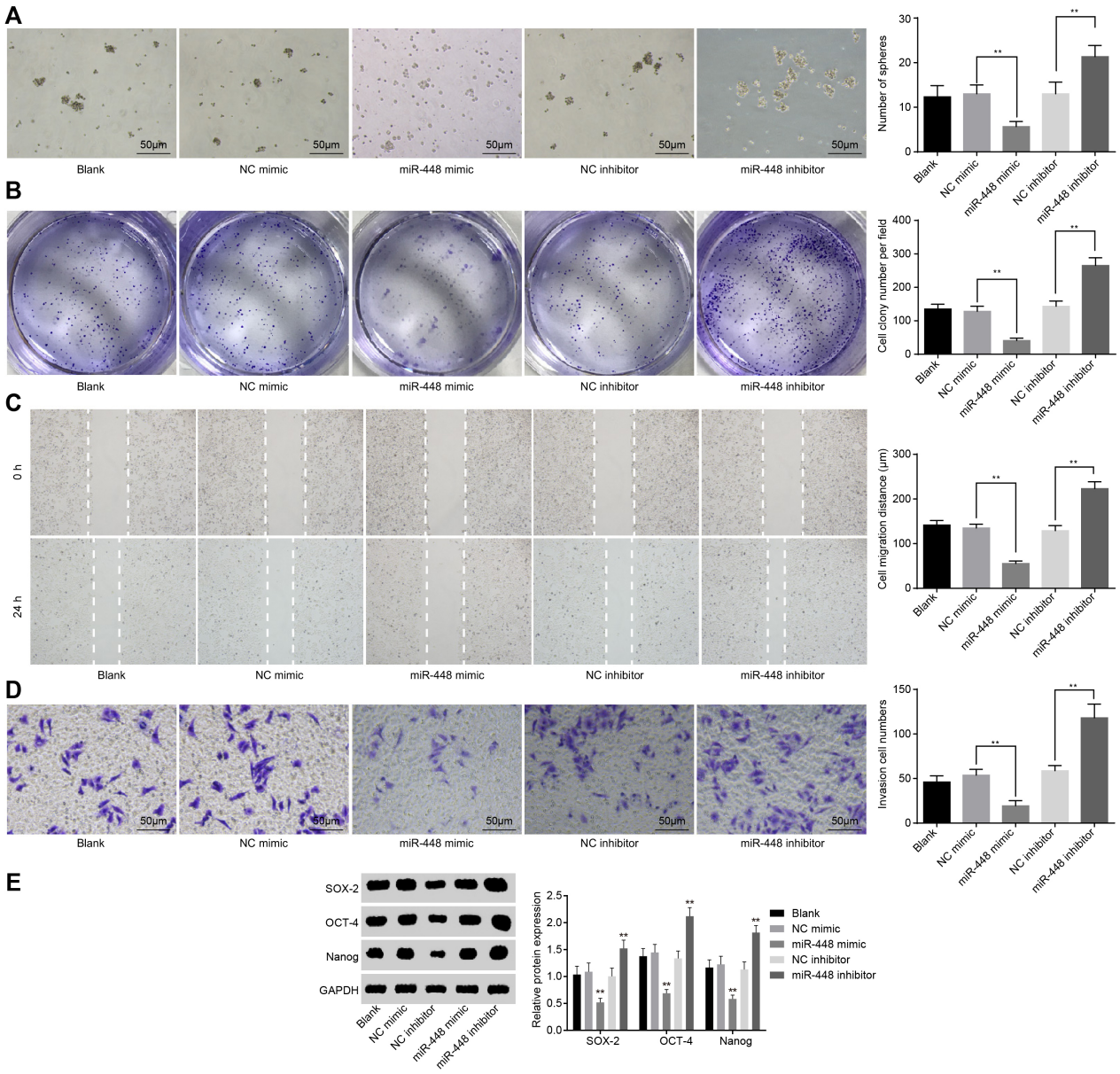

Figure 5. miR-448 inhibited pellet formation and invasion and migration of hepatoma tumor stem cells. Note: (A) Test result of stem cell pellet formation (×200 times); (B) clone formation test results; (C) Cell migration was detected by scratch test; (D) Transwell was used to detect cell invasion (×200 times). (E) WB was used to detect the expression of Sox4, Oct4 and Nanog in HCC stem cells of each group after transfection. Based on three independent experiments, the data were expressed as mean ± standard deviation. Independent sample t test was used for comparison between the two groups, and ** means $P < 0.05$ compared with NC.

($P < 0.05$). WB assay showed that compared with the Agomir NC group, the protein expression levels of stem cell markers SOX-2, OCT-4, Nanog and CD133 in the miR-448-Agomir group were significantly decreased ($P < 0.05$), indicating that the characteristics of stem cells in the miR-448-Agomir group were decreased. In addition, compared with the Agomir NC group, the expression of MAGEA6 in Mir-448-Agomir group was decreased, while the expression of P-AMPK was significantly increased ($P < 0.05$), which was consistent with the

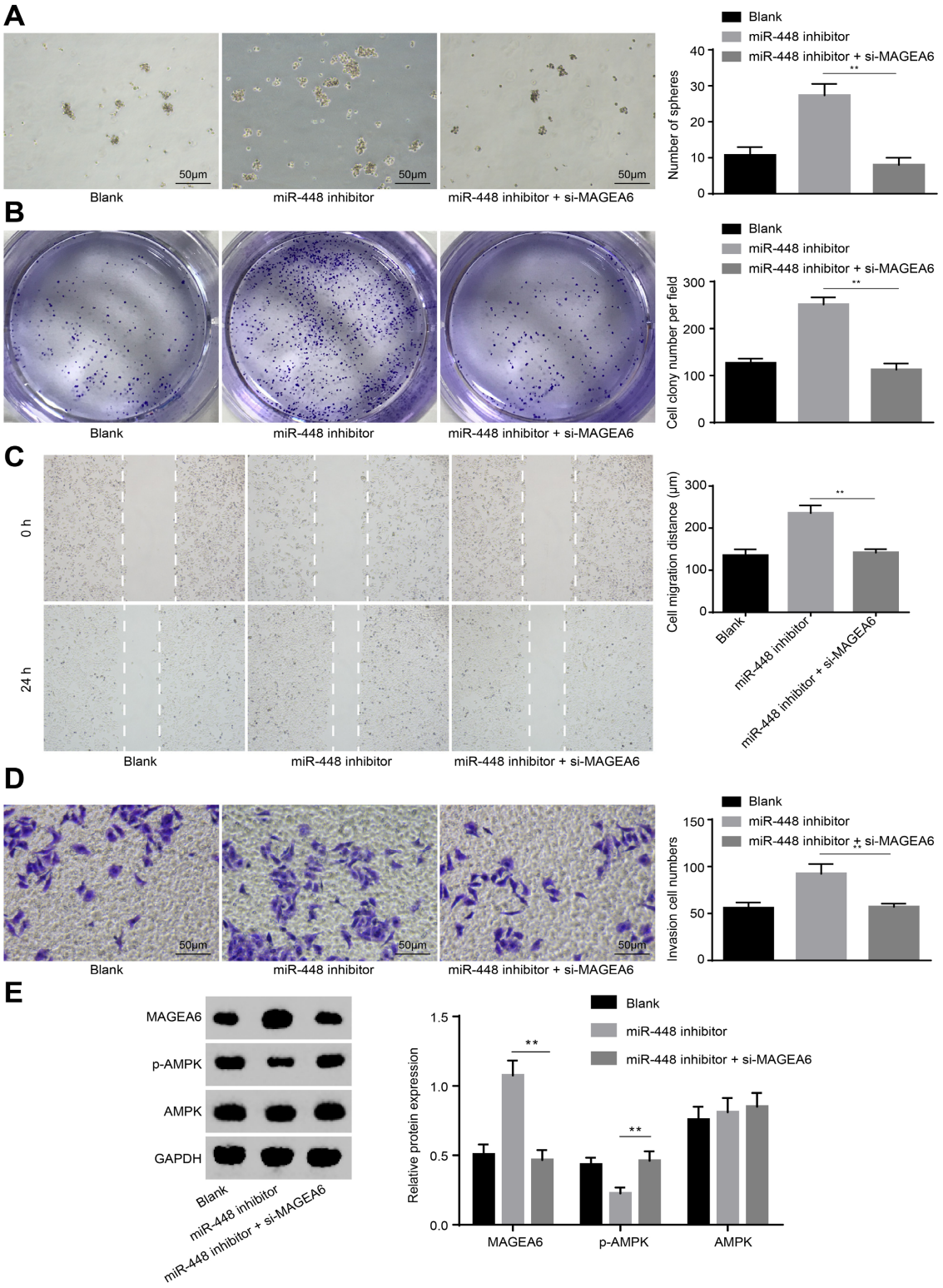

Figure 6. MAGEA6 silencing reverses the effect of miR-448 inhibitor on tumor. Note: (A) Test result of stem cell pellet formation (×200 times); (B) clone formation test results; (C) Cell migration was detected by scratch test; (D) Transwell was used to detect cell invasion (×200 times). (E) The expression of related proteins was detected by WB; Based on three independent experiments, the data were expressed as mean ± standard deviation. The analysis among multiple groups was performed by univariate variance statistics, ** indicated that compared with miR-448 inhibitor, $P < 0.05$.

results of *in vitro* experiments, namely, miR-448 activated AMPK signal by inhibiting the expression of MAGEA6. According to the above results, miR-448 can also inhibit tumor formation and stem cell characteristics *in vivo* (Figure 7).

4. Discuss

Liver cancer is considered to be one of the most common liver tumors, accounting for about 80% [19], although many diagnostic and therapeutic approaches are available for liver cancer, including surgical resection, liver transplantation, radioactive embolization, radiotherapy and molecular targeted therapy [20]. However, the lack of molecular markers suitable for the diagnosis and treatment of liver cancer remains an important problem. Therefore, it is very important to develop new therapeutic strategies and potential therapeutic targets for liver cancer patients [21] [22]. We investigated the effects of miR-448 on dryness maintenance and self-renewal of hepatocellular carcinoma stem cells. The results showed that MAGEA6 silencing or overexpression of miR-448 could inhibit the stem cells, proliferation, migration and invasion of hepatoma stem cells through AMPK signaling pathway. MAGEA6 is highly expressed in hepatocellular carcinoma stem cells, and

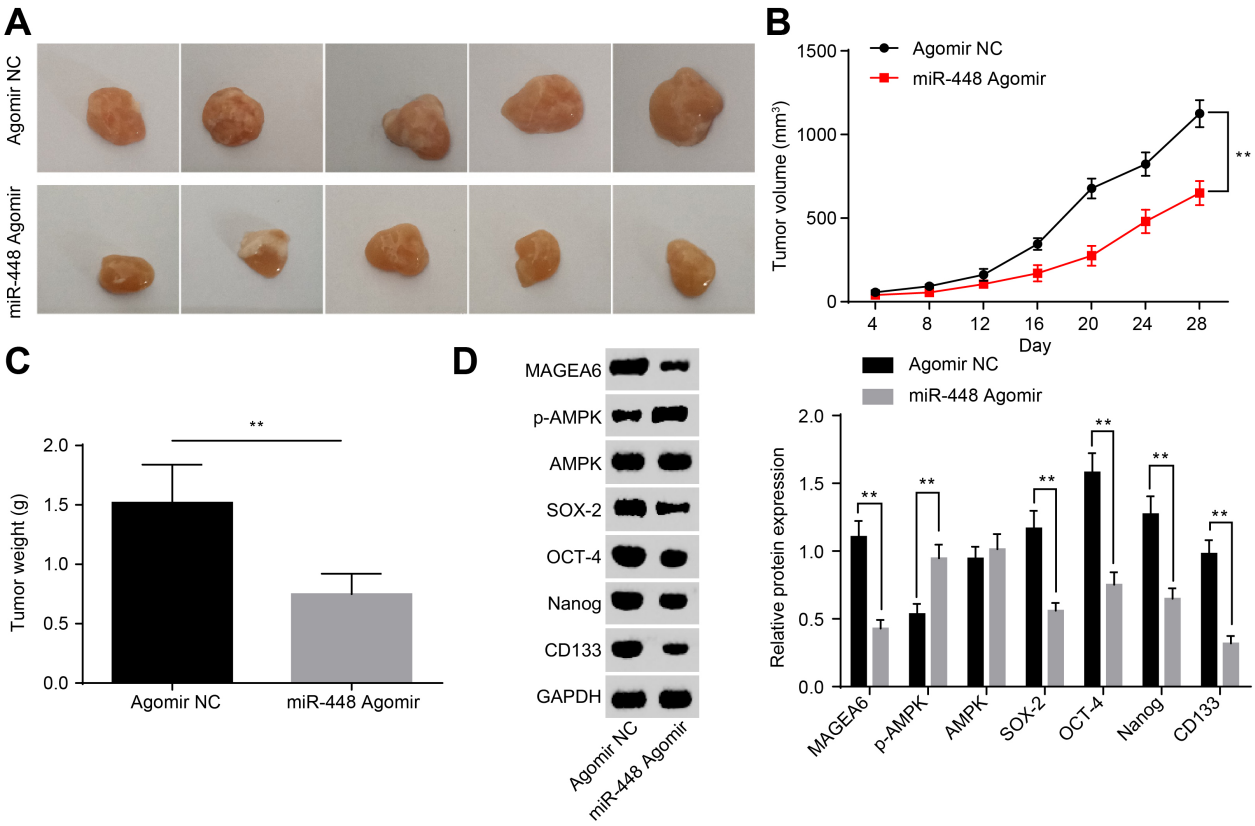

Figure 7. miR-448 inhibits tumor formation and stem cell characterization *in vivo*. Note: (A) Xenograft tumor of mouse liver cancer; (B) Tumor volume growth curve of xenograft tumors; (C) Tumor quality; (D) The expression of related proteins was detected by WB; Data are expressed as mean ± standard deviation. The comparison between the two groups was analyzed by the independent sample T-test statistical method, and the comparison between the two groups at different time points in Figure B was conducted by repeated measure analysis of variance. ** indicates that compared with Agomir NC group, $P < 0.05$. $n = 12$.

miR-448 has been shown to target MAGEA6, thereby affecting the progression of hepatocellular carcinoma. MAGEA9, a member of the MAGEA family, is highly expressed in laryngeal squamous cell carcinoma [23]. The expression of miR-448 is low in hepatocellular carcinoma tissues and inhibits the cell progression of hepatocellular carcinoma. Low expression of miR-448 can promote cell invasion by regulating ROCK2 in HCC [24]. Therefore, we can conclude that miR-448 targets MAGEA6 in liver cancer, which still needs further verification. Overexpression of miR-448 or silencing of MAGEA6 inhibited spherogenesis, colony formation, invasion and migration of hepatocellular carcinoma stem cells. Mirnas have been identified as a key part of HCC development, acting as cancer genes or tumor inhibitors in some malignancies (such as HCC) [25]. miR-448 has been downregulated in gastric and colorectal cancer, while up-regulated miR-448 inhibits cell proliferation, migration, invasion, and colony formation associated with these cancers [26]. In addition, Zhu *et al.* [27] have demonstrated that up-regulation of miR-448 can inhibit the invasion of HCC cells by targeting ROCK2 [28]. It is well known that bladder cancer stem cells with high expression level of MAGEA3 (one of the MAGE family such as MAGEA6) and CD133 are co-expressed positively [29]. All of these studies further demonstrated that miR-448 elevation or MAGEA6 silencing inhibited the biological properties of liver cancer stem cells. In addition, this study demonstrated that miR-448 activates the AMPK signaling pathway by targeting MAGEA6, thereby inhibiting spherogenesis, colony formation, invasion, and migration of hepatocellular carcinoma stem cells, as shown by the down-regulated expression of SOX-2, NANOG, OCT-4, and CD133. SOX-2, OCT-4, and NANOG have all been strongly validated as major regulators for maintaining dry cancer types [30]. MAGEA6 is a cancer-specific ubiquitin ligase that promotes the degradation of tumor inhibitor AMPK (Pan *et al.*, 2018). It is well known that high expression of miR-142-3p leads to significant reduction of breast cancer stem cell characteristics (such as CD44 and CD133) [31]. Sox2, Nanog and Oct4 are not only involved in self-renewal of stem cells, but also in cell migration and cancer invasion [32] [33]. CD133 has been identified as a potential marker of cancer stem cells in a variety of cancers, such as colorectal cancer [34]. Activation of AMPK signal plays a key role in regulating pancreatic cancer stem cells, and can also reverse the expression of SOX-2, OCT4 and NANOG [35] [36] [37] [38] [39]. Therefore, studies have shown that miR-448 negatively regulates the ability of MAGEA6 to activate AMPK signaling pathway, thereby inhibiting the spherical formation, colony formation, invasion and migration of hepatoma stem cells.

In conclusion, the elevation of miR-448 activates AMPK signaling by negatively regulating MAGEA6, thereby regulating stem cell maintenance and self-renewal mechanisms. miR-448 has good potential as a therapeutic target for liver cancer. It is imperative to further study its mechanism, and the research methods are various, which is helpful to the clinical application of liver cancer. In addition, we will further verify the presence of this AMPK signaling pathway

regulating migration and colony growth in HCC cell line Hep3b (not only stem cells) in further studies.

Foundation Project

Hainan Provincial Natural Science Foundation and Hainan Provincial Key Research and Development Program, No.: 821MS060.

Conflicts of Interest

The authors declare no conflicts of interest regarding the publication of this paper.

References

[1] Au, K.P. and Chok, K.S.H. (2018) Multidisciplinary Approach for Post-Liver Transplant Recurrence of Hepatocellular Carcinoma: A Proposed Management Algorithm. *World Journal of Gastroenterology*, **24**, 5081-5094. https://doi.org/10.3748/wjg.v24.i45.5081

[2] Chang, J.H., Au, H.K., Lee, W.C., Chi, C.C., Ling, T.Y., Wang, L.M. and Tzeng, C.R. (2013) Expression of the Pluripotent Transcription Factor OCT4 Promotes Cell Migration in Endometriosis. *Fertility and Sterility*, **99**, 1332-1339. https://doi.org/10.1016/j.fertnstert.2012.11.033

[3] El-Wahab, N.M., Rashed, H.G., El-Sherif, W.T., Sayed, S.K., Abd-Elmalek, M.O., Refaiy, A. and Mokhtar, A.A. (2017) Glypican-3 and Melanoma Antigen Genes 1 and 3 as Tumor Markers for Hepatocellular Carcinoma. *Egyptian Journal of Immunology*, **24**, 187-200.

[4] Gougelet, A. (2018) Exosomal MicroRNAs as a Potential Therapeutic Strategy in Hepatocellular Carcinoma. *World Journal of Hepatology*, **10**, 785-789. https://doi.org/10.4254/wjh.v10.i11.785

[5] Han, G., Zhang, L., Ni, X., Chen, Z., Pan, X., Zhu, Q. and Wang, X. (2018) MicroRNA-873 Promotes Cell Proliferation, Migration, and Invasion by Directly Targeting TSLC1 in Hepatocellular Carcinoma. *Cellular Physiology and Biochemistry*, **46**, 2261-2270. https://doi.org/10.1159/000489594

[6] Hardie, D.G. (2011) AMP-Activated Protein Kinase: A Cellular Energy Sensor with a Key Role in Metabolic Disorders and in Cancer. *Biochemical Society Transactions*, **39**, 1-13. https://doi.org/10.1042/BST0390001

[7] Jiang, W., Wang, S., Sun, Y., Jiang, Y., Yu, T. and Wang, J. (2017) Overexpression of MicroRNA-448 Inhibits Osteosarcoma Cell Proliferation and Invasion through Targeting of Astrocyte Elevated Gene-1. *Molecular Medicine Reports*, **16**, 5713-5721. https://doi.org/10.3892/mmr.2017.7249

[8] Katayama, Y., Maeda, M., Miyaguchi, K., Nemoto, S., Yasen, M., Tanaka, S. and Tanaka, H. (2012) Identification of Pathogenesis-Related MicroRNAs in Hepatocellular Carcinoma by Expression Profiling. *Oncology Letters*, **4**, 817-823. https://doi.org/10.3892/ol.2012.810

[9] Guo, Z.Y. and Zhu, Z.T. (2021) NCAPG is a Prognostic Biomarker Associated with Vascular Invasion in Hepatocellular Carcinoma. *European Review for Medical and Pharmacological Sciences*, **25**, 7238-7251.

[10] Li, B., Ge, L., Li, M., Wang, L., and Li, Z. (2016) miR-448 Suppresses Proliferation and Invasion by Regulating IGF1R in Colorectal Cancer Cells. *American Journal of Translational Research*, 3013-3022.

[11] Liao, Z.B., Tan, X.L., Dong, K.S., Zhang, H.W., Chen, X.P., Chu, L. and Zhang, B.X. (2018) miRNA-448 Inhibits Cell Growth by Targeting BCL-2 in Hepatocellular Carcinoma. *Digestive and Liver Disease*, **51**, 703-711. https://doi.org/10.1016/j.dld.2018.09.021

[12] Liu, M., Bamodu, O.A., Kuo, K.T., Lee, W.H., Lin, Y.K., Wu, A.T.H. and Tsai, J.T. (2018) Downregulation of Cancer Stemness by Novel Diterpenoid Ovatodiolide Inhibits Hepatic Cancer Stem Cell-Like Traits by Repressing Wnt/β-Catenin Signaling. *The American Journal of Chinese Medicine*, **46**, 891-910. https://doi.org/10.1142/S0192415X18500477

[13] Pan, S.J., Ren, J., Jiang, H., Liu, W., Hu, L.Y., Pan, Y.X. and Bian, L.G. (2018) MAGEA6 Promotes Human Glioma Cell Survival via Targeting AMPKα1. *Cancer Letters*, **412**, 21-29. https://doi.org/10.1016/j.canlet.2017.09.051

[14] Pineda, C.T., Ramanathan, S., Tacer, K.F., Weon, J.L., Potts, M.B., Ou, Y.H. and Potts, P.R. (2015) Degradation of AMPK by a Cancer-Specific Ubiquitin Ligase. *Cell*, **160**, 715-728. https://doi.org/10.1016/j.cell.2015.01.034

[15] Rupaimoole, R. and Slack, F.J. (2017) MicroRNA Therapeutics: Towards a New Era for the Management of Cancer and other Diseases. *Nature Reviews Drug Discovery*, **16**, 203-222. https://doi.org/10.1038/nrd.2016.246

[16] Mihaylova, M.M. and Shaw, R.J. (2011) The AMPK Signalling Pathway Coordinates Cell Growth, Autophagy and Metabolism. *Nature Cell Biology*, **13**, 1016-1023. https://doi.org/10.1038/ncb2329

[17] Morise, Z., Kawabe, N., Tomishige, H., Nagata, H., Kawase, J., Arakawa, S., Isetani, M. (2014) Recent Advances in the Surgical Treatment of Hepatocellular Carcinoma. *World Journal of Gastroenterology*, **20**, 14381-14392. https://doi.org/10.3748/wjg.v20.i39.14381

[18] Lv, J., Kong, Y., Gao, Z., Liu, Y., Zhu, P. and Yu, Z. (2018) LncRNA TUG1 Interacting with miR-144 Contributes to Proliferation, Migration and Tumorigenesis through Activating the JAK2/STAT3 Pathway in Hepatocellular Carcinoma. *The International Journal of Biochemistry & Cell Biology*, **101**, 19-28. https://doi.org/10.1016/j.biocel.2018.05.010

[19] Abbastabar, M., Sarfi, M., Golestani, A. and Khalili, E. (2018) lncRNA Involvement in Hepatocellular Carcinoma Metastasis and Prognosis. *EXCLI Journal*, **17**, 900-913.

[20] Attwa, M.H. and El-Etreby, S.A. (2015) Guide for Diagnosis and Treatment of Hepatocellular Carcinoma. *World Journal of Hepatology*, **7**, 1632-1651. https://doi.org/10.4254/wjh.v7.i12.1632

[21] Etik, O., Suna, N. and Boyacioglu, A.S. (2017) Management of Hepatocellular Carcinoma: Prevention, Surveillance, Diagnosis, and Staging. *Experimental and Clinical Transplantation*, **15**, 31-35.

[22] Sang, M., Wang, L., Ding, C., Zhou, X., Wang, B., Wang, L. and Shan, B. (2011) Melanoma-Associated Antigen Genes—An Update. *Cancer Letters*, **30**, 85-90. https://doi.org/10.1016/j.canlet.2010.10.021

[23] Han, L., Jiang, B., Wu, H., Zhang, S. and Lu, X. (2014) Expression and Prognostic Value of MAGE-A9 in Laryngeal Squamous Cell Carcinoma. *International Journal of Clinical and Experimental Pathology*, **7**, 6734-6742.

[24] Shen, L., Liu, L., Ge, L., *et al.* (2016) miR-448 Downregulates MPPED2 to Promote Cancer Proliferation and Inhibit Apoptosis in Oral Squamous Cell Carcinoma. *Experimental and Therapeutic Medicine*, **12**, 2747-2752. https://doi.org/10.3892/etm.2016.3659

[25] Sadri Nahand, J., Bokharaei-Salim, F., Salmaninejad, A., Nesaei, A., Mohajeri, F., Moshtzan, A. and Keyvani, H. (2018) microRNAs: Key Players in Virus-Associated Hepatocellular Carcinoma. *Journal of Cellular Physiology*, **234**, 12188-12225. https://doi.org/10.1002/jcp.27956

[26] Wu, X., Tang, H., Liu, G., Wang, H., Shu, J. and Sun, F. (2016) miR-448 Suppressed Gastric Cancer Proliferation and Invasion by Regulating ADAM10. *Tumor Biology*, **37**, 10545-10551. https://doi.org/10.1007/s13277-016-4942-0

[27] Zhu, H., Zhou, X., Ma, C., Chang, H., Li, H., Liu, F. and Lu, J. (2015) Low Expression of miR-448 Induces EMT and Promotes Invasion by Regulating ROCK2 in Hepatocellular Carcinoma. *Cellular Physiology and Biochemistry*, **36**, 487-498. https://doi.org/10.1159/000430114

[28] Li, Q.Q., Chen, Z.Q., Cao, X.X., *et al.* (2011) Involvement of NF-kappaB/miR-448 Regulatory Feedback Loop in Chemotherapy-Induced Epithelial-Mesenchymal Transition of Breast Cancer Cells. *Cell Death & Differentiation*, **18**, 16-25.

[29] Yin, B., Zeng, Y., Liu, G., Wang, X., Wang, P. and Song, Y. (2014) MAGE-A3 Is Highly Expressed in a Cancer Stem Cell-Like Side Population of Bladder Cancer Cells. *International Journal of Clinical and Experimental Pathology*, **7**, 2934-2941.

[30] Sengupta, S., Nagalingam, A., Muniraj, N., Bonner, M.Y., Mistriotis, P., Afthinos, A. and Sharma, D. (2017) Activation of Tumor Suppressor LKB1 by Honokiol Abrogates Cancer Stem-Like Phenotype in Breast Cancer via Inhibition of Oncogenic Stat3. *Oncogene*, **36**, 5709-5721. https://doi.org/10.1038/onc.2017.164

[31] Troschel, F.M., Bohly, N., Borrmann, K., Braun, T., Schwickert, A., Kiesel, L. and Greve, B. (2018) miR-142-3p Attenuates Breast Cancer Stem Cell Characteristics and Decreases Radioresistance in Vitro. *Tumor Biology*, **40**, 1-10. https://doi.org/10.1177/1010428318791887

[32] Song, Y., Xiao, L., Fu, J., Huang, W., Wang, Q., Zhang, X. and Yang, S. (2014) Increased Expression of the Pluripotency Markers Sex-Determining Region Y-box 2 and Nanog Homeobox in Ovarian Endometriosis. *Reproductive Biology and Endocrinology*, **12**, Article No. 42. https://doi.org/10.1186/1477-7827-12-42

[33] Siu, M.K., Wong, E.S., Kong, D.S., Chan, H.Y., Jiang, L., Wong, O.G. and Cheung, A.N. (2013) Stem Cell Transcription Factor NANOG Controls Cell Migration and Invasion via Dysregulation of E-cadherin and FoxJ1 and Contributes to Adverse Clinical Outcome in Ovarian Cancers. *Oncogene*, **32**, 3500-3509. https://doi.org/10.1038/onc.2012.363

[34] Lee, Y.M., Yeo, M.K., Seong, I.O. and Kim, K.H. (2018) Nuclear Expression of CD133 Is Associated with Good Prognosis in Patients with Colorectal Adenocarcinoma. *Anticancer Research*, **38**, 4819-4826. https://doi.org/10.21873/anticanres.12792

[35] Sun, L., Cao, J., Chen, K., Cheng, L., Zhou, C., Yan, B. and Xu, Q. (2019) Betulinic Acid Inhibits Stemness and EMT of Pancreatic Cancer Cells via Activation of AMPK Signaling. *International Journal of Oncology*, **54**, 98-110. https://doi.org/10.3892/ijo.2018.4604

[36] Vara, D., Salazar, M., Olea-Herrero, N., Guzman, M., Velasco, G. and Diaz-Laviada, I. (2011) Anti-Tumoral Action of Cannabinoids on Hepatocellular Carcinoma: Role of AMPK-Dependent Activation of Autophagy. *Cell Death & Differentiation*, **18**, 1099-1111. https://doi.org/10.1038/cdd.2011.32

[37] Wu, Y., Li, Q. and Chen, X.Z. (2007) Detecting Protein-Protein Interactions by Far Western Blotting. *Nature Protocols*, **2**, 3278-3284. https://doi.org/10.1038/nprot.2007.459

[38] Yamashita, T. and Wang, X.W. (2013) Cancer Stem Cells in the Development of

Liver Cancer. *Journal of Clinical Investigation*, **123**, 1911-1918. https://doi.org/10.1172/JCI66024

[39] Ye, X., Xie, J., Huang, H. and Deng, Z. (2018) Knockdown of MAGEA6 Activates AMP-Activated Protein Kinase (AMPK) Signaling to Inhibit Human Renal Cell Carcinoma Cells. *Cellular Physiology and Biochemistry*, **45**, 1205-1218. https://doi.org/10.1159/000487452